ENCYCLOPEDIA OF MATERIALS SCIENCE AND ENGINEERING

Editor-in-Chief

MICHAEL B. BEVER

ENCYCLOPEDIA OF MATERIALS SCIENCE AND ENGINEERING

Volume 6
R–S

Editor-in-Chief
MICHAEL B. BEVER
Massachusetts Institute of Technology, USA

PERGAMON PRESS
OXFORD · NEW YORK · TORONTO · SYDNEY · FRANKFURT

U.K.

U.S.A.

w Park,

CANADA

2J 1P9.

AUSTRALIA

544.

FEDERAL REPU
OF GERMANY

many

JAPAN — Pergamon Press Ltd., 8th Floor,
Matsuoka Central Building, 1–7–1 Nishishinjuku,
Shinjuku-ku, Tokyo 160, Japan

BRAZIL — Pergamon Editora Ltda., Rua Eça de Queiros, 346,
CEP 04011, São Paulo, Brazil

PEOPLE'S REPUBLIC OF CHINA — Pergamon Press, Qianmen Hotel, Beijing,
People's Republic of China

First edition 1986

Library of Congress Cataloging in Publication Data

Main entry under title:
Encyclopedia of materials science and engineering.
Includes bibliographies.
1. Materials—Dictionaries. I. Bever, Michael B.
(Michael Berliner). II. Massachusetts Institute of Technology
TA402.E53 1986 620.1'1'0321 85–23192

British Library Cataloguing in Publication Data

Encyclopedia of materials science and engineering
1. Materials science—Dictionaries
I. Bever, Michael B.
620.1'1'0321 TA402

ISBN 0–08–022158–0 (set)

Distributed in North and South America by The MIT Press,
Cambridge, Massachusetts

Computer typeset by Page Bros. (Norwich) Ltd.
Printed in Great Britain by A. Wheaton & Co. Ltd., Exeter.

ENCYCLOPEDIA OF
MATERIALS SCIENCE
AND
ENGINEERING

HONORARY EDITORIAL ADVISORY BOARD

SUBJECT EDITORS

Willard D. B. Bascom
Hercules Incorporated, USA

Harold Berger
Industrial Quality Incorporated, USA

Michael B. Bever
Massachusetts Institute of Technology, USA

Jack M. Blakely
Cornell University, USA

Richard J. Brook
University of Leeds, UK

Robert W. Cahn
Clare Hall, UK

Donald D. Carr
Indiana Geological Survey, USA

Gilbert Y. Chin
AT&T Bell Laboratories, USA

Philip C. Clapp
University of Connecticut, USA

Theodore F. Cooke
Textile Research Institute, USA

Stephen M. Copley
University of Southern California USA

William D. Davenport
University of Arizona, USA

Larry G. DeShazer
Spectra Technology, USA

George E. Dieter
University of Maryland, USA

Thomas S. Ellis
General Motors Research Laboratories, USA

Anthony G. Evans
University of California at Santa Barbara, USA

Brian R. T. Frost
Argonne National Laboratory, USA

John W. Glomb
Westvaco Corporation, USA

Evan H. Greener
Northwestern University Dental School, USA

W. Lincoln Hawkins
Plastics Institute of America, USA

Norman Herz
University of Georgia, USA

Walter R. Hibbard, Jr.
Virginia Polytechnic Institute and State University, USA

Frank E. Karasz
University of Massachusetts, USA

Anthony Kelly
University of Surrey, UK

Thomas B. King†
Massachusetts Institute of Technology, USA

Jerome Kruger
Johns Hopkins University, USA

Robert A. Laudise
AT&T Bell Laboratories, USA

Henry Leidheiser, Jr.
Lehigh University, USA

Eric Lifshin
General Electric Corporate Research and Development, USA

Margaret L. A. MacVicar
Massachusetts Institute of Technology, USA

James E. Mark
University of Cincinnati, USA

Koichi Masubuchi
Massachusetts Institute of Technology, USA

Malcolm G. McLaren
Rutgers University, USA

Fred Moavenzadeh
Massachusetts Institute of Technology, USA

David D. Mulligan
Westvaco Corporation, USA

J. Merle Nielsen
General Electric Company, USA

Eli M. Pearce
Polytechnic University, USA

David J. Perduijn
Nederlandse Philips Bedrijven BV The Netherlands

Benjamin W. Roberts†
General Electric Corporate Research and Development, USA

Philip Ross
National Academy of Sciences, USA

Arno P. Schniewind
University of California at Berkeley, USA

Gilbert R. Speich
Illinois Institute of Technology USA

Leo A. Stuijts†
Philips Research Laboratories The Netherlands

Jack H. Wernick
Bell Communications Research, USA

Jack H. Westbrook
General Electric Materials Information Services, USA

James L. White
University of Akron, USA

CONTENTS

R

Radial Distribution Function

A thorough understanding of the behavior and properties of a material is usually based on a description of its structure, that is, the spatial arrangement of its constituent atoms. Much effort has been devoted, therefore, to the formulation of experimentally accessible structural descriptions and their measurement. The radial distribution function is one such description, which is particularly relevant to noncrystalline materials.

1. Definition

In general, the atomic arrangement in a material can be described in terms of three-dimensional pair-density functions $\rho_{ij}(\boldsymbol{r})$, which are proportional to the probability that there is a j-type atom at vector position $\boldsymbol{r}$ from an average i-type atom. However, if the interatomic vectors have no preferred orientations when averaged over the sample as a whole, the density functions are spherically symmetrical. Then, it is useful to consider the averaged scalar quantity $4\pi r^2\rho(r)\,dr$, which is the total number of atom centers in a spherical shell (of radius r and thickness dr) about an atom, averaged over all atoms. The function $4\pi r^2\rho(r)$ is called the radial distribution function (RDF). Denoting the average density of atoms per unit volume as ρ_a, it is often convenient to refer to a differential radial distribution $D(r) = 4\pi r^2[\rho(r) - \rho_a]$, or to $G(r) = D(r)/r$, or to a relative density $g(r) = \rho(r)/\rho_a$. In a multiconstituent material the total RDF can be expressed in terms of the separate distributions $\rho_i(r)$ around each type of atom:

$$4\pi r^2\rho(r) = 4\pi r^2 \sum_{i=1}^{n} x_i\rho_i(r) \qquad (1)$$

where

$$\rho_i(r) = \sum_{j=1}^{n} \rho_{ij}(r),$$

x_i is the fraction of each atom type and n is the number of different species. Not all terms are independent, since $x_i\rho_{ij}(r) = x_j\rho_{ji}(r)$.

Figure 1 shows the differential radial distribution for pure liquid aluminum. The peaks reflect the most prevalent interatomic distances. The value of $\rho(r)$ is zero below the nearest-neighbor peak because each atom has a finite size and excludes the volume immediately around itself. The range of clearly nonrandom correlations (~20 Å, $\sim 7r_1$) is of the same order as for many liquids and glasses, but correlation ranges of more than 40 Å have also been reported for specific liquids.

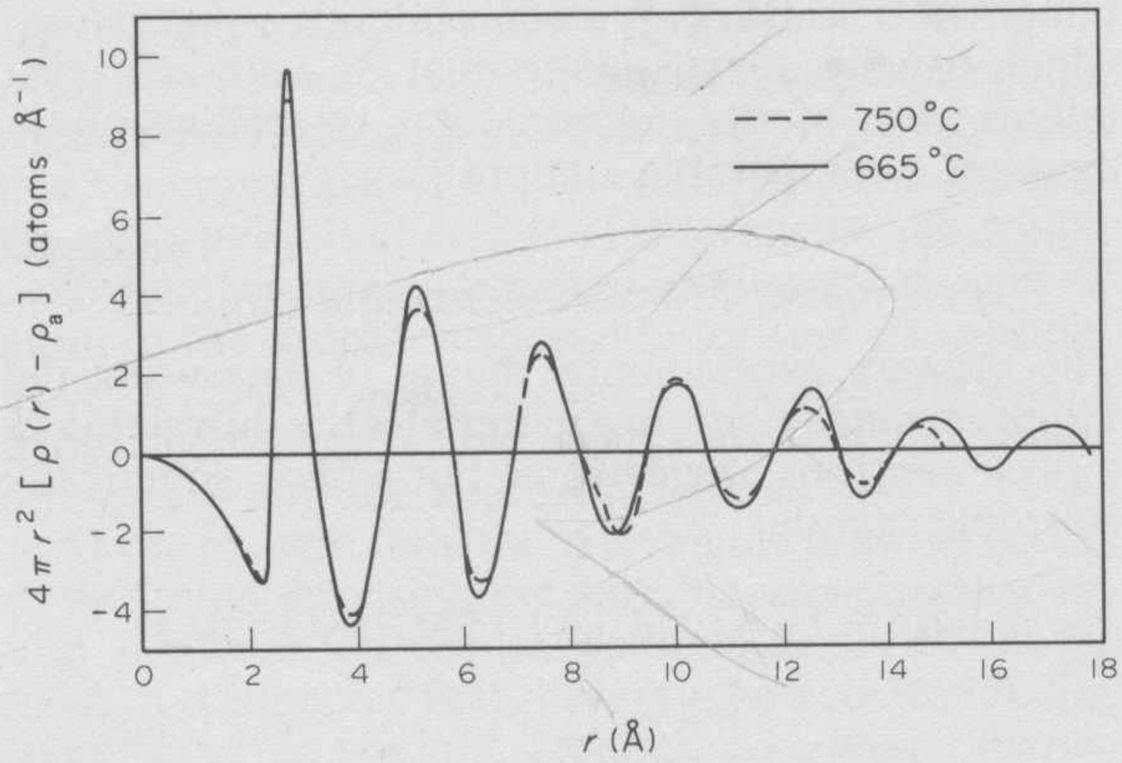

Figure 1
Radial density functions $4\pi r^2[\rho(r) - \rho_a]$ for liquid aluminum (after Fessler et al. 1966. © American Physical Society, New York. Reproduced with permission)

2. General Aspects

The RDF is most important as a structural description when the material is inherently spherically isotropic on a dimensional scale less than the minimum necessary for experimental study. Such materials include gases, liquids, glasses and other "amorphous" solids, such as isotropic, noncrystalline polymers. The concept can also be applied to crystalline materials or to oriented polymers by forming randomized samples for measurement (e.g., polycrystalline powders).

Diffraction techniques provide direct access to the RDF for pure materials. Functions closely related to the total RDF can be measured for multielement materials; the partial density functions are accessible in special instances, especially for the case of a material with only two different elements.

The RDF represents only the spherically averaged topological order; it contains no explicit information about the relative orientation of interatomic vectors or the identity of atom pairs. The averaging processes cannot be analytically reversed, which is to say that the three-dimensional structure cannot be uniquely determined from the RDF. In certain cases, however, different interatomic bonds are well resolved in real space at characteristic distances. Using the areas of identified peaks to determine coordination numbers, it is sometimes possible to infer at least the near-neighbor configuration. More

BVOL6-A*

generally, an experimental RDF can serve as a check on a proposed model structure.

Experimentally determined RDFs of noncrystalline materials are generally consistent with the presumption that local bonding, including distances, angles, anisotropies and species preferences, is maintained in a low-energy, nonrandom configuration, which usually approximates that of a known crystalline form of the material, if a crystalline phase exists at a comparable composition.

3. *Experimental Measurements and Analysis*

The primary experimental means of measuring the atomic arrangements in a material is the diffraction of x rays, neutrons or electrons. For a pure, spherically isotropic sample:

$$I(K) = f^2(K) - f^2(K) \int 4\pi r^2[\rho(r) - \rho_a)] \times \frac{\sin Kr}{Kr}\, dr \qquad (2)$$

where the integral is over the irradiated sample and $I(K)$ is the coherently diffracted intensity per atom (exclusive of the structure-independent intensity peak at $K = 0$), in units of the intensity scattered by a single electron; $K = (4\pi \sin\theta)/\lambda$ (the magnitude of the diffraction vector); $\theta =$ is one-half the angle of scattering; λ is the wavelength of the radiation; and $f(K)$ is the atomic scattering amplitude.

With a pure material, the differential RDF is directly determined, in principle, through Fourier transformation of Eqn. (2):

$$4\pi r^2[\rho(r) - \rho_a] = r\int_0^\infty K\left[\frac{I(K) - f^2(K)}{f^2(K)}\right]\sin Kr\, dK \qquad (3)$$

In practice, limits on the experimentally accessible region of K ($K_{max} < \infty$) cause uncertainty about sharp details in $\rho(r)$.

For a multiconstituent material:

$$I(K) = \langle f^2(K)\rangle + \sum_i \sum_j x_i f_i(K) f_j(K) \times \int 4\pi r^2 \rho_{ij}(r) \frac{\sin Kr}{Kr}\, dr - \langle f(K)\rangle^2 \int 4\pi r^2 \rho_a(r) \frac{\sin Kr}{Kr}\, dr \qquad (4)$$

where $f_i(K)$ is the scattering amplitude of the ith type atom, with atomic fraction x_i; and

$$\langle f^2(K)\rangle = \sum_i^n x_i f_i^2(K)$$

$$\langle f(K)\rangle^2 = \left|\sum_i^n x_i f_i(K)\right|^2 \qquad (5)$$

For the diffraction of neutrons by the atomic nuclei the individual scattering factors are constant and the quantities $w_{ij}(K) = f_i(K)f_j(K)/\langle f(K)\rangle^2$ are therefore independent of K. Then, a direct solution can be found for a modified distribution function in which each partial distribution function is weighted by the relative scattering power for the particular atomic pair:

$$4\pi r^2[\rho'(r) - \rho_a] = 4\pi r^2 \left|\left[\sum_i \sum_j x_i w_{ij} \rho_{ij}(r)\right] - \rho_a\right| = r\int_0^\infty K\left[\frac{I(K) - \langle f^2\rangle}{\langle f\rangle^2}\right]\sin Kr\, dK \qquad (6)$$

For x rays and electrons, the $w_{ij}(K)$ functions differ in shape as well as magnitude, so the same transform of the data yields only an approximation; each weighted function, $4\pi r x_i w_{ij}(0)\rho_{ij}(r)$, actually appears as the convolution of its true shape with the Fourier transform of $w_{ij}(K)/w_{ij}(0)$. Usually, however, this approximation (the "experimental" RDF) yields at least a good starting point for an "exact" analysis in which the experimental functions are systematically matched to functions computed on the basis of trial structural models.

In Fig. 2, experimental RDF data are shown for a number of gold–tin liquid alloys, measured just above

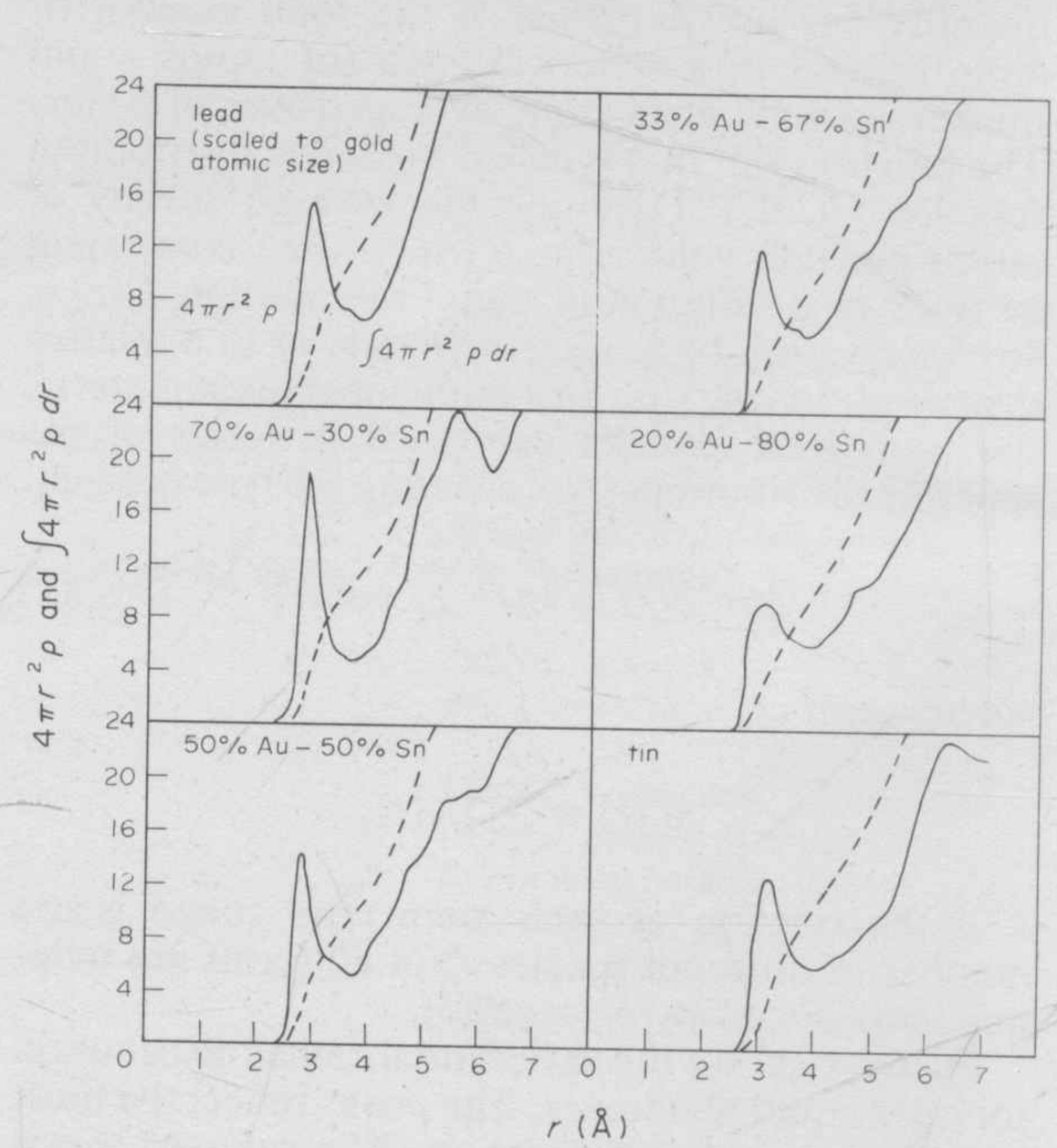

Figure 2
Total density functions $4\pi r^2\rho(r)$ and integrals $\int^r 4\pi r^2\rho(r)\, dr$ for gold–tin alloys, tin and lead (after Kaplow et al. 1966. © Gordon and Breach, New York. Reproduced with permission)

the liquidus temperatures. In this case the two $f(K)$'s are similar in shape, so the functions are not seriously distorted. These data have been interpreted as indicating compositional short-range order.

The possibility of varying the weight of the contribution of particular constituents to $4\pi r^2\rho(r)$ by varying the relative scattering powers can be used to gain additional information. For a two-constituent material, for example, it is possible (albeit difficult) to determine experimentally all three independent partial distribution functions (or particular combinations of them). Variation of relative scattering power can be accomplished by using different radiations, by varying the radiation wavelength (anomalous dispersion), by using different isotopes or elements which behave the same in the material, or (in magnetic materials) by the use of polarized neutrons.

In this context, three particular combinations of the partial density functions have been shown to be convenient for binary materials. The difference function $x_A x_B[\rho_A(r) - \rho_B(r)] = \rho_{NC}(r)$ represents the atomic size and coordination differences. The function $x_A\rho_A(r) + x_B\rho_B(r) = \rho_{NN}(r)$ is the density of atoms of both types at distance r. The function $\rho_{cc}(r)$ is referred to as the compositional (or chemical) order function for binary materials, and is equal to $x_B\rho_A(r) + x_A\rho_B(r) - \rho_{AB}(r)/x_B$.

Figure 3 shows the differential functions $G(r) = 4\pi r[\rho(r) - \rho_a]$, $4\pi r\rho_{cc}(r) = G_{cc}(r)$, $4\pi r\rho_{NC}(r) = G_{NC}(r)$ and $4\pi r\rho_{NN}(r) = G_{NN}(r)$ for a $Ni_{35}Zr_{65}$ alloy glass in which the nearest-neighbor nickel and zirconium bonds are just resolved. These results were all derived from x-ray data and point to a preference for unlike (Ni–Zr) first neighbors, as indicated by the minimum in $G_{cc}(r)$ at $r = 2.68$ Å.

Mention should also be made of an additional experimental technique, extended x-ray absorption fine structure (EXAFS). The fine structure of the x-ray absorption immediately following an absorption edge depends on the distribution of atoms around an atom of the species responsible for that absorption. Thus, information analogous to the separate $\rho_i(r)$'s is obtained directly, but it appears that the results are sensitive to the nearest neighbors only.

At the present time there is rapidly growing access to new high-intensity and variable-wavelength x-ray and neutron sources at national facilities in the USA. It is expected that there will be a corresponding increase in the volume, accuracy and detail of structural data for noncrystalline materials.

See also: Crystal Structure Determination

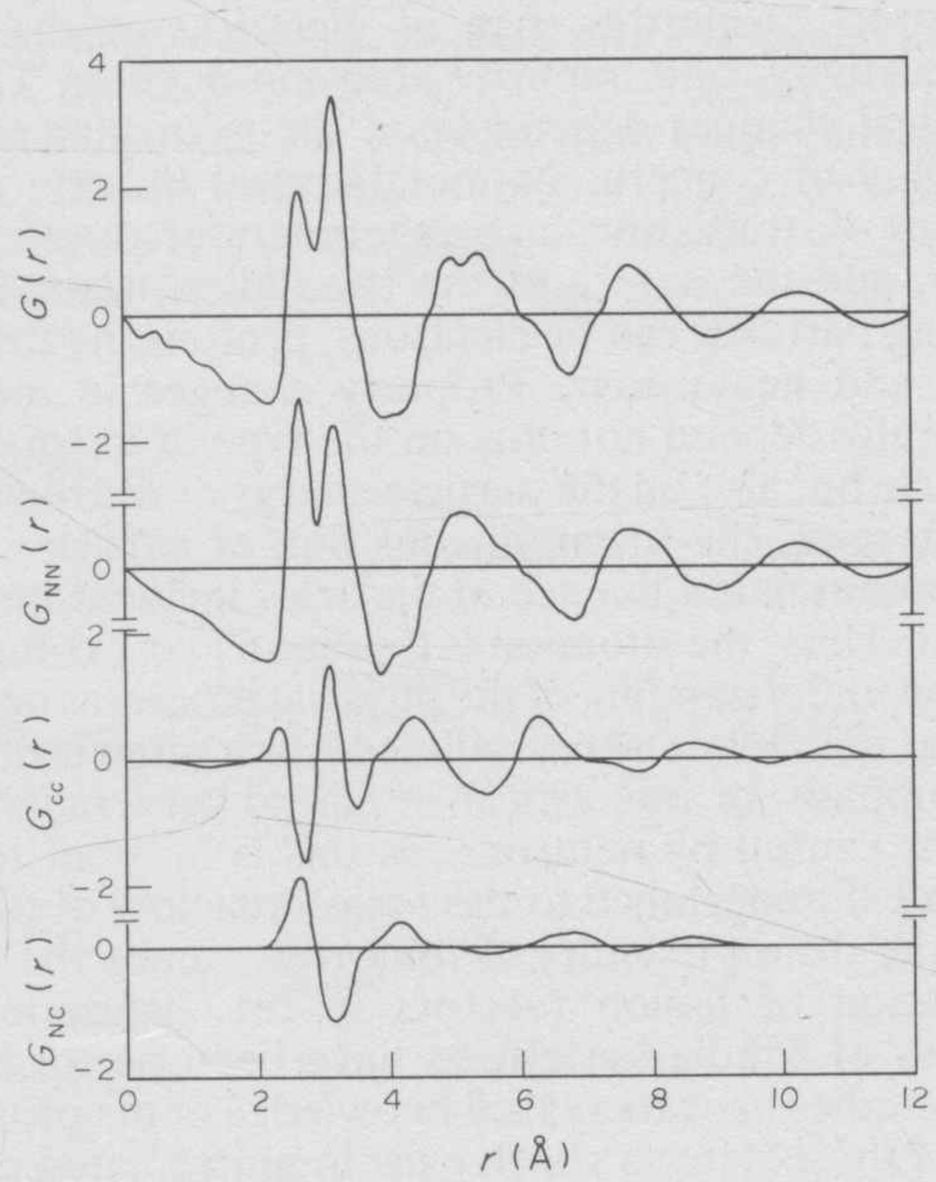

Figure 3
Atomic distribution function $G(r)$ of an amorphous $Ni_{35}Zr_{65}$ alloy. Also shown are the distribution functions $G_{NN}(r)$, $G_{NC}(r)$ and $G_{cc}(r)$ (after Wagner and Ruppersberg 1981. © International Atomic Energy Agency, Vienna. Reproduced with permission)

Bibliography

Azároff L V, Kaplow R, Kato N, Weiss R J, Wilson A J C, Young R A 1974 *X-Ray Diffraction.* McGraw-Hill, New York, pp. 79–138

Fessler R R, Kaplow R, Averbach B L 1966 Pair correlations in liquid and solid aluminum. *Phys. Rev.* 150: 34–43

Kaplow R, Strong S L, Averbach B L 1966 Local order in liquid alloys. In: Cohen J B, Hilliard J E (eds.) 1966 *Local Atomic Arrangements Studied by X-Ray Diffraction.* Gordon and Breach, New York, pp. 159–77

Wagner C N J 1980 Diffraction analysis of metallic, semiconducting and inorganic glasses. *J. Non-Cryst. Solids* 42: 3–22

Wagner C N J, Ruppersberg H 1981 Neutron and x-ray diffraction studies of the structure of metallic glasses. *At. Energy Rev.* Suppl. 1: 101–41

Warren B E 1969 *X-Ray Diffraction.* Addison–Wesley, Reading, Massachusetts, pp. 116–50

Wright A C, Leadbetter A J 1976 Diffraction studies of glass structure. *Phys. Chem. Glasses* 17: 122–45

R. Kaplow†; J. B. Cohen

Radial Forging

Radial forging is a metalworking process in which a workpiece is reduced in thickness by being fed into and through reciprocating dies (usually two, four or six radially aligned dies) as the total die closure is controlled to produce the desired product contour. This contour is circular if the workpiece is rotated, or square, rectangular, hexagonal, and so on, depending on the number of dies and the rotation.

Workpieces are either solid or hollow (typically for mandrel-forging tubular products) and may be held from one end, both ends alternately, or on centers during the entire forging cycle. The dies are connected to rams of presses, either mechanically or hydraulically powered, which provide a continuous small-amplitude stroke and a contouring capability by controlled net displacement of the rams.

Radial forging evolved from swaging in the late 1940s to reduce noise level, to improve contouring capabilities for both internal and external forms, and to facilitate productivity and automation.

1. Basic Design

There are three basic machine designs: (a) radially aligned presses, for machines with two or more dies per impression; (b) off-center loading of a split die holder moving in a slideway, for machines with two dies for each of one or two impressions achieved with two-axis motion of the feed mechanism; and (c) die closure by loading through a pivot, for machines with two dies for a single impression.

The common features of the press designs are: (a) cycling of the dies through a small amplitude (about 2% of the maximum size capacity of the machine) at frequencies in the range of 200–1500 Hz (inversely proportional to press capacity); (b) die closure superimposed on the die cycling (controlled by the feed motion); and (c) independently controlled workpiece rotation.

Auxiliary features include various combinations of chucks and/or headstocks and tailstocks, mandrel capabilities, special mandrel-cycle control for combined rifling and chambering of gun barrels for four-die machines, automatic induction heating, and automatic loading and unloading.

2. Typical Products

Radial forging has become a significant production practice in the processing of railroad car, automobile and truck axles; ingot breakdown; bottles for containing gases; rifle, shotgun and artillery barrels; contoured shafts and precision tubes; contoured products for forging preforms; and oil-field couplings. Radial forging is internationally recognized as the most advanced production forging practice for railroad car axles and gun barrels.

3. Forging Tolerances and Metallurgical Considerations

Tolerances and surface quality are functions of the preform feed per blow or die closure and are therefore economic considerations. Rifling and chambering in a single machine cycle can produce bore surfaces with a finish of less than 0.25 μm, diameter control to less than +5 μm, outer diameter control to less than ±50 μm and straightness of less than 2×10^{-4}.

Radial forging can result in a spiralled microstructure, and significant residual stresses and Bauschinger effects during subsequent cold working. Machine parameters and tooling design can be used to minimize or control these material responses.

See also: Swaging; Metallic Tube Production; Metals Processing and Fabrication: An Overview

Bibliography

Kralowetz B 1963 Radial forging comes over here. *Am. Mach.* September: 124

Selwood R W 1970 *GFM Precision Mechanical, Hydraulic and Continuous Forging Machines*, SME Technical Paper MF 70–591. Society of Manufacturing Engineers, Dearborn, Michigan

A. L. Hoffmanner

Radiation Effects in Metals and Alloys

Bombardment with energetic particles produces changes in the physical properties of metals or alloys. The physical property changes of technological interest include dimensional changes, embrittlement, enhanced creep, segregation or phase change, sputtering at surfaces, surface modification, changes in transport properties such as electrical or thermal conductivity, and impurity atom production. These physical changes depend upon the particular metal or alloy of concern, its metallurgical history, conditions of irradiation such as temperature and stress state, and the nature of the irradiation itself. Irradiating particles can be electrons, protons, neutrons, light and heavy ions. Property changes in metals generally depend not only on the type of irradiation particle but also on the particle energy or distribution of energies, the instantaneous flux of particles and the accumulated fluence of particles incident on the metal. Thus, the situation is frequently very complex and an understanding of the physical processes occurring at the atomic or crystalline level is often lacking.

Emphasis in this article is placed on irradiation effects caused by neutrons, as this is of great technological importance to the fission reactors of today and the fusion reactors of tomorrow. Since the first operation of fission reactors in the 1940s, many studies of irradiation effects have been performed; such studies have increased knowledge of the properties of those defects which exist in unirradiated crystalline solids and can be produced in a controlled fashion by irradiation. However, much of what has been learned so far is applicable only to a few pure metals and, to a lesser extent, simple alloy systems; complete understanding of the behavior of more complex systems awaits further research.

1. Defects Produced by Irradiation

Most solid metals and alloys are crystalline, with the constituent atoms forming a regular periodic lattice in three dimensions. Defects in the periodic lattice are nearly always present in some concentration. They are often loosely classified on the basis of their dimensionality as point, line, plane and volume defects. All of these defects can be found in unirradiated metals, but they can often be produced in much higher concentration by irradiation.

The simplest defect produced in metals by irradiation is the Frenkel defect, consisting of a self-interstitial atom and a vacancy. If a lattice atom receives sufficient energy from a bombarding particle, usually 10–100 eV, this atom will recoil from its lattice site and it, or a neighboring atom, will be displaced into an interstitial site between regular lattice sites (see *Lattice Defect Production During Irradiation*). Thus, a self-interstitial atom is formed along with a vacant lattice site (vacancy), that is, two point defects appear (Fig. 1a). This Frenkel defect is stable only at very low temperatures (<20 K) in many metals. Therefore, irradiation to study both interstitial and vacancy point defects is often performed at very low temperature, usually in liquid helium (4.2 K). At temperatures exceeding 100 K, interstitials are mobile in most metals and alloys, and at some higher temperature, usually near or somewhat above room temperature, the vacancy is mobile. When either defect becomes mobile, it migrates through the crystal lattice until it annihilates with its opposite kind, clusters with the same kind of defect or an impurity atom, or is absorbed by a defect sink such as a dislocation (line defect), a grain boundary or surface (planar defect) or a cavity (volume defect) (see *Recovery of Low-Temperature Irradiation Damage*).

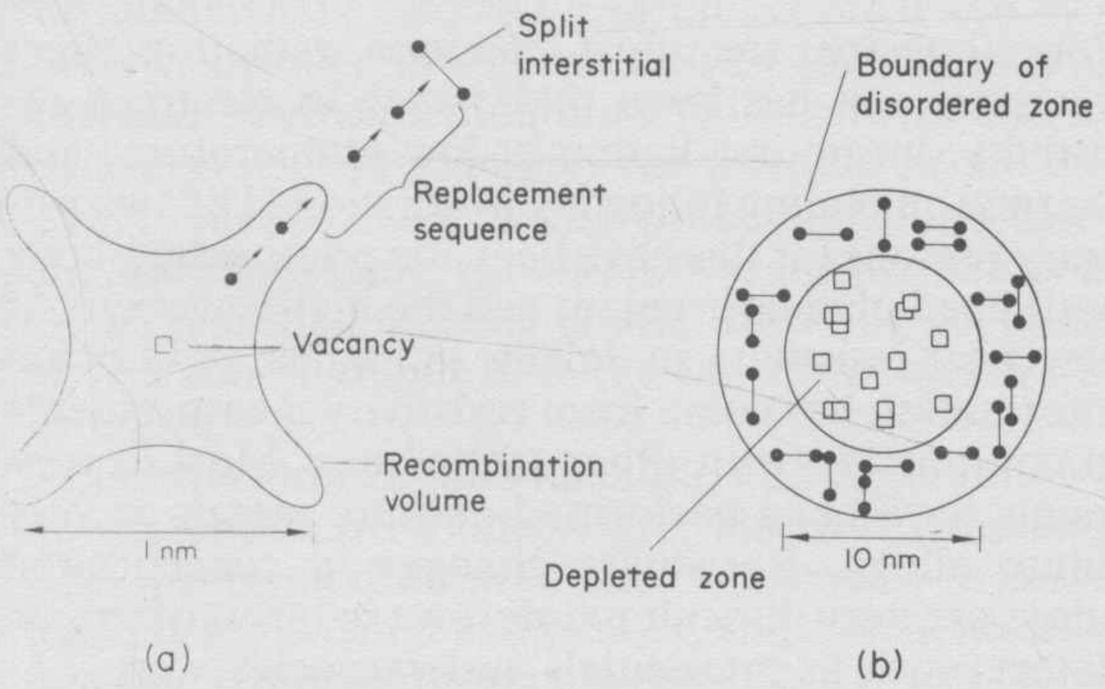

Figure 1
(a) A 50 eV displacement event with a single interstitial produced at the end of a replacement sequence; (b) a 30 keV displacement event with many defects produced in a cascade (typical of fast-neutron damage)

If the recoil energy of the primary knock-on atom (PKA) is large (>10 keV), this atom initiates a collision cascade involving many atoms. A defect cascade is thus produced which includes several hundred interstitials and vacancies in a rather small region of the crystal lattice, of the order of 10 nm in diameter. All features of the collision and defect production process in this cascade are not well understood at present. It has long been believed, and supported by computer model calculations, that the resultant defect cascade has an interior region of high vacancy concentration, often called a depleted zone, which is surrounded by a cloud of interstitials (Fig. 1b). Only recently have direct experimental results begun to reveal some aspects of cascade structure. This is a rather important area of investigation, since large defect cascades are the dominant damage produced by fission and fusion neutron irradiation.

Although this simple description of the structure of a defect cascade is appropriate at very low temperatures (near absolute zero), it does not indicate the complexities that can result at higher temperatures. When defect cascades are formed at temperatures sufficiently high for defect migration, the interstitials and vacancies from a single cascade can annihilate each other, cluster, condense on a plane to form a dislocation loop, or freely migrate to react with other existing defects. What happens depends primarily on the material and the temperature. Detailed knowledge of this process is seriously lacking for virtually all materials. It is generally believed that the vacancy clusters or dislocation loops produced at cascade sites contribute to irradiation hardening and embrittlement. The freely migrating interstitials and vacancies which are absorbed at sinks, such as dislocations and cavities, contribute to irradiation-enhanced creep and void growth, respectively. The details of these processes are largely unknown, but they are again strongly dependent on the material and temperature (see *Electron Microscope Observations of Defect Clusters, Voids and Bubbles*).

At very high PKA recoil energies this simple description of defect production in cascades must be amended to include the formation of subcascades. As the recoil energy increases above approximately 50 keV, the defect cascade, rather than simply getting larger, divides into separately identifiable subcascades. These subcascades are closely spaced and each is typical of a 25–30 keV primary recoil event. The frequent production of subcascades is typical of irradiation of metals by fusion neutrons.

Defect production is believed to be largely unaffected by the addition of small concentrations of impurities (<1 at.%) to a pure metal. However, impurities can have a pronounced effect upon the fate of migrating defects. This is largely through trapping of migrating interstitials or vacancies by certain impurities. This can change the balance of

steady-state concentrations of interstitials and vacancies and thus change their effect upon macroscopic properties.

For concentrated alloys, which include most metals with engineering applications, present lack of knowledge on the atomic scale is so serious as to preclude even a simple description of defect production, defect migration or the resulting defect structures. For most concentrated alloys only the eventual macroscopic effects upon the properties of irradiated alloys are known.

2. *Types of Irradiation*

It is appropriate here to consider briefly the different possible irradiating particles, their sources and the different types of damage that they create in metals. Accelerators provide the energetic electrons, protons, light and heavy ions used in charged-particle irradiation (see *Particle Accelerators in Materials Research*). Electron and proton irradiations produce predominantly isolated point defects and are used to study fundamental properties and interactions of point defects. Heavy-ion irradiation, with energies between 10 and 100 keV, is often performed to study the properties of defect cascades. However, a disadvantage of heavy-ion bombardment is the short range of the ions, typically 100 nm or less. Light-ion irradiations produce some combination of isolated Frenkel pairs and defect cascades over longer ranges.

Technologically, the most important irradiating particle is the neutron, and the source of most neutrons is the fission process in a reactor. Neutrons produced by fission of ^{235}U typically have an energy of 1 MeV and can produce defect cascade damage in metals and alloys. In a thermal reactor, fission neutrons are slowed or moderated to energies typical of reactor temperatures (<1 eV). These thermal neutrons are capable of producing defects in materials by the (n,γ) reaction: neutron absorption and atomic recoil from prompt γ emission. The atom recoil energies during this process are fairly low, and isolated and small clusters of Frenkel defects are usually produced. In addition, each reaction produces one transmuted atom (impurity). One of the unique aspects of either fission or thermal neutron irradiation is that the damage events are uniformly distributed in most materials at thicknesses of the order of centimeters. This fact, among others, makes the simulation of neutron damage by ion irradiation exceedingly difficult or impossible.

Neutron damage in core components of a fast breeder reactor is primarily caused by fission neutrons, whereas the damage in core components of a thermal reactor is a mixture of that caused by fission and thermal neutrons. In the pressure vessel of a thermal reactor, damage due to (n,γ) processes dominates. In the nuclear fuel itself (uranium or plutonium alloys), and in the fuel cladding to some extent, damage is mainly produced by the fragments from the fissioned atom rather than by the neutron. The fission fragments are very energetic (100 MeV) heavy ions. Fission fragment damage is characterized by defect cascades formed along a dense track some μm in length (see *Radiation Effects on Nuclear Fuels*).

Recently, some interest has focused on the neutron damage that can be expected in a fusion reactor. The fusion reactor contains a dense plasma of hydrogen isotopes and produces neutrons with energies near 14 MeV. The containment vessel wall will be bombarded with these neutrons together with light ions from the plasma. The difference between damage caused by 1 MeV and 14 MeV neutrons is currently being studied. Generally, a 14 MeV neutron irradiation of a metal creates elastic recoils with higher energies and thus produces more subcascade damage. Also, the higher-energy neutrons are more likely to produce nonelastic events such as (n,p) or (n,α). These reactions cause hydrogen and helium production internally in a metal or alloy and can seriously affect its dimensional and mechanical properties.

The superconducting magnets in the fusion reactor are shielded and the distribution of neutron energies is expected to be similar to that found in a fission reactor. Thus, neutron damage to the magnet materials for a fusion reactor can be studied by using the neutrons from a fission reactor. Such studies have indicated that potentially serious problems due to neutron damage in the superconducting magnet materials can be expected after a few years of operation. This is a good example of an area where low-temperature (4.2 K) studies are not just useful for a fundamental understanding but necessary from an engineering point of view (see *Radiation Effects on Superconductors*).

3. *Fundamental Experiments*

For 30 years, the most common radiation-effect measurement has been the change in electrical resistivity during irradiation at low temperatures and thermal annealing following irradiation. The two primary reasons for this have been the relative simplicity and speed of measurement and the high sensitivity of electrical resistivity to defects in metals. Additional information has come from resistivity measurements in conjunction with other techniques. Most experiments have been performed on pure metals or very dilute alloys. Resistivity changes in concentrated alloys are very difficult to interpret in terms of simple defects such as interstitials and vacancies.

In electron irradiation of metal single crystals, by varying the energy (usually in the range 300 keV to 2 MeV) the minimum or threshold energy for defect production can be determined for different crystallographic directions. There are "easy" and "hard"

directions for defect production in a single crystal. For many pure metals, the minimum threshold energy is in the range 10–100 eV. The directional variation of the threshold energy is an important quantity in the understanding of defect production and interatomic potentials (see *Lattice Defect Production During Irradiation*).

Electron irradiation of metals exhibits a decreasing defect production rate as the defect concentration increases (usually measured by resistivity changes). This radiation annealing yields a measurement of spontaneous recombination volume: the volume around an isolated vacancy or interstitial in which another defect of opposite kind cannot be placed without spontaneous recombination of both defects (Fig. 1a). This volume, which has been measured to be about 100 atomic volumes, limits the maximum damage concentration.

The thermal annealing of defects produced at 4.2 K by electron irradiation has demonstrated single interstitial migration at very low temperatures (<100 K) and single vacancy migration near room temperature in many metals. Other annealing processes are attributed to close Frenkel-pair annihilation, the release of previously trapped interstitials or vacancies, and the disappearance of migrating interstitials or vacancies at defect sinks such as dislocations, grain boundaries and surfaces. Dilute alloys have been especially useful in studying in a controlled fashion the trapping of interstitials at impurities (see *Recovery of Low-Temperature Irradiation Damage*).

Electron irradiation cannot produce large defect cascades which are of primary importance in fission and fusion neutron damage. Defect cascades are produced by neutron and heavy-ion bombardments and are often studied by resistivity measurements at low temperature. Varying the bombarding ion mass between light and heavy has revealed the difference in the character of damage produced by electrons and by heavy ions. Also, recent advances in neutron dosimetry have allowed a careful comparison of resistivity damage rates produced by low-temperature ion and neutron irradiations from several different accelerators and reactors. An increase in the PKA energy results in a less than proportional increase in the number of interstitials and vacancies. This is due to increased lattice agitation, resulting in greater defect annihilation within the cascade at higher PKA energies.

Comparison of the annealing of defects following low-temperature neutron and electron irradiations also displays differences due to cascades. When the defects are created in cascades, there is an increased tendency during thermal annealing for like defects to form clusters that remain stable to higher temperatures. Also, the vacancies in the cascade center may collapse to a plane of vacancies or, in effect, a dislocation loop. These effects are especially important during higher-temperature irradiation of metals and alloys that are used in reactor technology, but have also been observed (by transmission electron microscopy and diffuse x-ray scattering) to occur at very low temperatures (<50 K) in some metals.

A major limitation to all resistivity experiments is the uncertainty in the resistivity per Frenkel pair. Determination of the Frenkel-pair resistivity is possible only by the simultaneous measurement of an additional defect property from which the number of defects can be determined. This has now been performed on several pure metals. An additional uncertainty is the constancy of the Frenkel-pair resistivity when the defect is in a cluster or dislocation loop.

Diffuse x-ray scattering measurements following electron irradiation at 4.2 K have shown that the ⟨100⟩ split interstitial is the stable defect in several face-centered-cubic (fcc) metals, while the ⟨110⟩ split interstitial is stable in several body-centered-cubic (bcc) metals. A split interstitial consists of two atoms sharing one lattice site with their axis along the direction given. Simultaneous resistivity and diffuse x-ray measurements have demonstrated that the Frenkel-pair resistivity in several metals is apparently unchanged by clustering of up to tens of defects.

Similar measurements have been performed on several metals following fission-neutron irradiation at 4.2 K. These are very difficult experiments, which can be performed presently at only three laboratories in the world. Results on several metals suggest that the interstitials within the cascade are found in clusters even at 4.2 K (see *X-Ray and Neutron Diffuse Scattering Studies of Radiation-Induced Defects*).

An even more direct "picture" of individual defect cascades has been obtained in two metals (tungsten and platinum) with the atomic resolution of the field-ion microscope. Following ion irradiation, a defect cascade is viewed in the field-ion microscope one atomic plane at a time while the atomic planes are field-evaporated. In this way the vacancies and interstitials of a defect cascade have been located for some tens of cascades. The technique is limited to those metals that are fairly easily imaged in the field-ion microscope, and the number of cascades is limited by the experimental time needed to examine each. Nevertheless, these results are the only direct picture of a cascade and are extremely valuable as such. They have shown the cascade to contain a vacancy-rich central region with the interstitials at unusually large distances from the vacancies, a result that may be somewhat unique to tungsten (see *Field-Ion Microscopy: Observation of Radiation Effects*).

Transmission electron microscopy has recently contributed to the direct "picture" of defect cascades through the images of disordered zones (or volumes) associated with defect cascades in an ordered alloy of Cu_3Au. These disordered zones are formed by the atomic interchanges (replacements) that occur during the displacement process, and give a picture

of the shapes and sizes of cascades produced by fission and fusion neutrons (Fig. 1b). More traditional electron microscopy has centered on the study of dislocation loops produced by neutron, ion and electron irradiations. Electron irradiation has been investigated in situ in the high-voltage electron microscope, where the electron beam itself is of sufficient energy to create Frenkel defects in many metals and alloys (see *Electron Microscope Observations of Defect Clusters, Voids and Bubbles*).

In addition to their study in the electron microscope, ordered alloys have been investigated with several other experimental techniques to reveal fundamental mechanisms of radiation damage. Measurement with the electron microscope, resistivity and magnetization are all quite sensitive to the disordering of ordered atoms rather than displacements (Frenkel pairs). Although replacements are an integral part of the displacement process, they are not observable in the crystal lattice of a pure metal but are revealed as disorder in an ordered alloy. The number of disordered atoms in Cu_3Au and Ni_3Mn (both ordered alloys) following neutron irradiation at 4.2 K has been measured by resistivity changes, and the character of the disorder has been measured by magnetization changes in Ni_3Mn. Experiments on thermal-neutron irradiation of Ni_3Mn have directly demonstrated the importance of replacement collision chains as a defect production mechanism at low recoil energies (<500 eV) (Fig. 1a). Fast-neutron irradiation of Ni_3Mn reveals that replacement chains are not effective in transporting interstitials far from the cascade periphery at high recoil energies (~30 keV) in this fcc alloy.

Some of the most recent experiments have employed nuclear techniques to probe the defects at an atomic level. Experiments using the hyperfine interaction in Mössbauer emission have investigated impurity trapping of interstitials in several dilute alloys. Positron annihilation and perturbed angular correlation measurements have been used to study vacancy agglomeration into microscopic voids in the metal lattice (see *Positron Annihilation Spectroscopy of Defects in Metals*).

Finally, the guidance and understanding offered by the results of computer model and analytical theory calculations must be emphasized. Many experiments have been suggested by such calculations. Analytical theory followed by computer calculations of recoil events in a crystal lattice provided the first suggestion of the low-energy defect production mechanism of the replacement collision sequence. The channelling of an incident atom between two lattice planes was first suggested by binary-collision calculations. The structure of the interstitial in fcc and bcc metals was first suggested by computer calculations. Analytical theory has been especially useful in understanding radiation effects at a surface such as sputtering (erosion). It has been the combination of this theoretical work and critical experiments that has provided the present understanding of fundamental radiation damage mechanisms (see *Lattice Defect Production During Irradiation*; *Computer Simulation of Radiation-Induced Defects*).

4. Dimensional Changes under Irradiation

Fundamental understanding of the irradiation phenomena important in dimensional and mechanical property changes (see Sect. 5) is considerably less than for the cases considered above. The fundamental studies referred to above have mainly employed low irradiation fluences ($\leq 10^{18}$ neutrons per cm^2, $E_n > 0.1$ MeV) on either pure metals or very dilute alloys, and often at low temperatures such as 4.2 K. Most of the effects to be discussed presently require or occur noticeably at high fluences ($>10^{20}$ neutrons per cm^2), at high temperatures (0–700 °C), in concentrated alloys or with combinations of these.

Dimensional changes during irradiation include: swelling, a net overall volume increase; growth, found in the highly anisotropic metal uranium; radiation-enhanced creep, the time-dependent plastic deformation of a material under external stress; and sputtering, the loss of material at a surface during irradiation. These dimensional changes can be very important technologically, with potentially severe economic impact on any reactor design that must allow for them. Any contribution that research can make to control these poorly understood phenomena will probably aid in the design of alloys or systems that minimize these effects and thus produce substantial savings in costs in future fission and fusion reactor designs.

The swelling of a material under neutron irradiation was a rather recent and unexpected discovery, because it had always been supposed that radiation effects would be absent if the irradiation temperature was above that at which vacancies readily migrate. It was believed that mutual recombination of nearly all vacancies and interstitials would occur with no permanent structural changes. However, swelling of the order of 10% was discovered in high-fluence fast-neutron irradiation of stainless steels, and a quite intense experimental program was begun in an attempt to understand the mechanisms involved.

Void swelling apparently results from an imbalance of the steady-state concentrations of vacancies and interstitials produced during the irradiation. This imbalance is believed to be due to certain sinks for point defects, such as dislocations, that have a slight bias toward the absorption of interstitials. This results in an excess of vacancies that can agglomerate into voids rather than be annihilated at interstitials or sinks. A number of empirical factors are evident but not understood such as sensitivity of void growth to nickel and chromium concentrations in the stainless

steels and the role in void nucleation of helium gas internally generated by inelastic neutron interactions. A number of experimental techniques have been employed to investigate swelling, beyond simple dimensional and density measurements. The most common of these has been transmission electron microscopy, which gives information on void concentrations and sizes for different irradiation fluxes and temperatures (Fig. 2). Ion simulation techniques have been employed in most of these studies because ion irradiation can simulate in hours the necessary neutron fluences that would take years of irradiation to produce. However, there are difficulties in correlating simulation experiments with neutron irradiation. Recent techniques of investigation include x-ray and neutron diffraction and positron annihilation measurements. Swelling in a complex alloy is not understood on a fundamental basis, in spite of a large amount of empirical data that has identified high- and low-swelling alloys (see *Swelling in Irradiated Metals and Alloys*).

Irradiation growth is similar to swelling in that dimensional changes occur, but without an overall volume change. This is possible in highly anisotropic materials, which during irradiation expand in one direction while contracting in another. Growth in uranium and zirconium is of great importance because of their use in fission fuels and fuel cladding. One mechanism suggested to explain growth is the formation of dislocation loops with preferred orientation in an anisotropic metal.

Irradiation-enhanced creep has been observed in several metal alloys and has potentially serious consequences in structural components of nuclear reactors. Experiments to understand this phenomenon are exceedingly difficult and thus few. Theoretical mechanisms have been proposed, usually including the climb of dislocations by absorption of the point defects created during irradiation.

A dimensional change at an irradiated surface can be produced by sputtering (erosion by ejection of material). For neutron irradiation this process has received attention, because of the possibility of excessive first-wall erosion in a fusion reactor. It was concluded, however, that 14 MeV neutron sputtering was of secondary importance compared with sputtering by light plasma ions. Ion sputtering for other applications, and as a subject of study itself, has been an active area of research. Over a broad range of projectile (ion) and target masses, sputtering is well understood within a presently accepted theoretical framework. However, incomplete understanding exists for light-ion sputtering and very-heavy-ion sputtering. Care must be exercised in the application of this theory to the sputtering of alloys; individual components can sputter at different rates, thus changing the near-surface composition and requiring long-range atomic migration to achieve equilibrium sputter fluxes (see *Sputtering*).

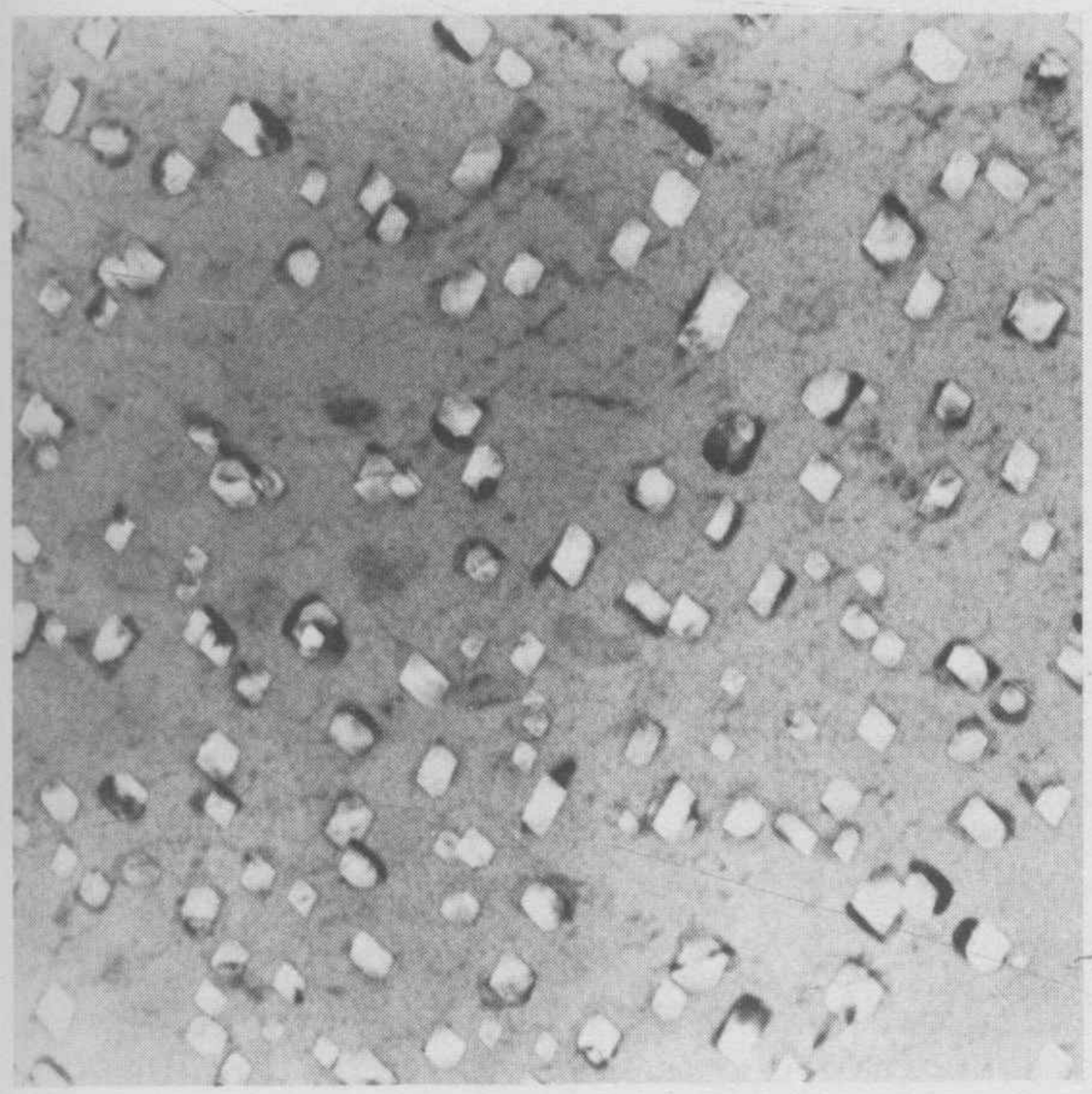

Figure 2
Transmission electron micrograph of an 18%Cr-8%Ni-1%Si-Fe alloy after 1 MeV electron irradiation at 500 °C; the bright rectilinear areas indicate voids and the dark edges a silicon-rich precipitate due to irradiation-induced segregation

5. Mechanical Property Changes During Irradiation

Closely related to the effects discussed in the previous sections are irradiation-produced changes in the mechanical properties of metals and alloys. Such properties as hardness and fracture mode can be affected by microstructural changes produced by neutron irradiation. These changes can have serious consequences for the structural components of fission and fusion reactors. For example, the lifetime of the pressure vessel in light-water reactors is dictated by embrittlement. A gradual upward shift of the ductile–brittle transition temperature takes place with accumulated neutron fluence and must be taken into account in reactor design. A better understanding of this process and improved alloy design could ease these design restrictions, with great economic benefits.

In a pure metal like copper, it is believed that irradiation hardening results from the interaction of irradiation-produced dislocation loops with gliding dislocations. The dislocation loops provide a uniform distribution of obstacles to be overcome by the gliding dislocation, with a resultant increase in flow or yield stress. In a heavily neutron-damaged metal, the dislocations are observed to glide in distinct channels, and plastic deformation and failure become quite

inhomogeneous. At somewhat elevated temperatures (500 °C) in austenitic steels, the irradiation produces voids and a complex dislocation structure. Failure takes place along channels at high stress levels but intergranularly at low stress levels. Also, an effect in some alloys is the irradiation-enhanced or -induced precipitation of a second phase which produces barriers to dislocation glide, similar to normal precipitation hardening. There is no detailed understanding of the interactions between dislocations and the various types of barriers to their motion. In fact, the study of irradiation effects upon mechanical properties will potentially aid in the understanding of the behavior of these properties in the absence of irradiation. In a fast-reactor spectrum, especially that of a fusion reactor, the transmutation production of helium also contributes to changes in mechanical behavior under irradiation. For example, the helium can segregate to grain boundaries and increase the probability of brittle intergranular fracture of the metal (see *Radiation Effects on Plastic Deformation and Fracture*).

6. *Alloy Redistribution Effects During Irradiation*

Local changes in alloy composition occur under virtually all conditions of irradiation. The effects include the radiation-induced segregation of alloy constituents to defect sinks, re-solution or mixing at a boundary of a second phase, and radiation-induced (or -enhanced) second-phase precipitation. These effects involve radiation-enhanced diffusion.

Radiation-enhanced diffusion in a metal is a result of the production of a high concentration (relative to the thermally produced concentration) of interstitials and vacancies by irradiation and the high mobility of at least one species of defect. All processes controlled or affected by diffusion are thus usually accelerated by the irradiation (see *Radiation Effects on Diffusion*). Additional diffusion mechanisms may be created. The process is complex in an alloy because several types of vacancies and interstitials are possible and several migration modes may exist. Radiation-enhanced diffusion in a pure metal or dilute alloy is difficult to study experimentally, owing to the complexities of the problem. Even less work has been accomplished on concentrated alloys.

During fast-neutron or heavy-ion irradiation the defect cascades themselves may contribute to the re-solution of second-phase precipitates by a cascade mixing process at the phase boundaries. This process of dynamic mixing of the atoms in the cascade volume is closely related to the disordering of ordered alloys by cascades. While an equilibrium second phase may grow or disappear during irradiation, a non-equilibrium second-phase precipitate may also be produced (see *Ion Implantation Metallurgy*). This somewhat unusual and as yet unexplained phenomenon has been observed by electron microscopy.

Finally, a recently discovered and now actively studied area is radiation-induced segregation to defect sinks. This effect has been observed by transmission electron microscopy in samples that have been heavily irradiated by ions or neutrons (Fig. 2). It is believed that fluxes of migrating defects interacting with alloy constituent atoms cause a redistribution of the constituents and precipitation of the second phase at defect sinks such as dislocations, voids or a surface. This effect is interdependent with changes in mechanical properties, void growth and dimensional changes, and surface modification and sputtering.

See also: Neutron Interactions with Matter; Ion Bombardment of Materials

Acknowledgement

The authors acknowledge financial support from the US Department of Energy under Contract No. W-31-109-ENG-38.

Bibliography

Journal of Nuclear Materials 69/70, 1978. Proceedings of the International Conference on Properties of Atomic Defects in Metals

Journal of Nuclear Materials 108/109, 1982. Proceedings of the International Conference on Neutron Irradiation Effects in Solids

Nolfi F V Jr (ed.) 1983 *Phase Transformations During Irradiation*. Applied Science, New York

Peterson N L, Harkness S D (eds.) 1976 *Radiation Damage in Metals*. American Society for Metals, Metals Park, Ohio

Robinson M T, Young F W (eds.) 1976 *Proc. Int. Conf. Fundamentals Aspects of Radiation Damage in Metals*, ERDA, CONF-751006-P1 and P2. US Energy Research and Development Association, Washington, DC

Seeger A, Schumacher D, Schilling W, Diehl J (eds.) 1970 *Proc. Int. Conf. Vacancies and Interstitials in Metals*. North-Holland, Amsterdam

Takamura J, Doyama M, Kiritani M (eds.) 1982 *Proc. 5th Int. Conf. Point Defects and Defect Interactions in Metals*. University of Tokyo Press, Tokyo

Thompson M W 1969 *Defects and Radiation Damage in Metals*. Cambridge University Press, Cambridge

M. A. Kirk; R. C. Birtcher

Radiation Effects on Diffusion

The diffusion of lattice atoms takes place via the motion of point defects, especially of vacancies; by creating point defects, radiation increases diffusion at temperatures where the defects are mobile. Further enhancement of atomic diffusion occurs owing to the mixing of atoms in collision cascades, fission spikes or thermal spikes. The radiation-enhanced diffusion coefficient D_{rad} is small, usually $<10^{-18}$ m^2 s^{-1}, although the relative enhancement can be very large.